Available online at www.sciencedirect.com

ScienceDirect

Procedia Engineering 160 (2016) 143 – 150

Procedia Engineering

www.elsevier.com/locate/procedia

XVIII International Colloquium on Mechanical Fatigue of Metals (ICMFM XVIII)

Fatigue performance of hybrid steel samples with laser sintered implants

L.M.S. Santos[a], J.A.M. Ferreira[a], J.D. Costa[a], C. Capela[a,b]*

[a] CEMUC, University of Coimbra, Department of Mechanical Engineering, Rua Luís Reis Santos, 3030-788, Coimbra, Portugal.
[b] Instituto Politécnico de Leiria, ESTG, Department of Mechanical Engineering, Morro do Lena – Alto Vieiro, 2400-901 Leiria, Portugal.

Abstract

Laser sintering metal has recently been used in the manufacture of metallic structural hybrid components comprising two different materials obtained by two distinct technological processes. This process allows to obtain productivity gains reducing sintering time and hence the cost. In current study it was used a machined substrate in which it is built by sintering the remaining part. The purpose of present work was to study the effect of the substrate material and interface microstructure on the fatigue performance under constant and variable block loadings. The sintering laser parts were manufactured in maraging steel AISI 18Ni300, while the substrates of hybrid specimens were produced alternatively in two materials: the steel for hot work tools AISI H13 and the stainless steel AISI 420. Fatigue strength will be quantified in terms of S - N curves. The results show that tensile properties of sintered specimens and of the hybrid parts was similar. Fatigue strength for short lives, of the sintered specimens and hybrid parts was quite similar. However, the fatigue strength of hybrid parts tends to decrease, for long lives, when compared with single sintered specimens. The fatigue tests under block loadings leads to indicate that the application of Miner's law is adequate to predate fatigue life in hybrid components with sintered implants, despite having been observed a tendency to be conservative for long life.

Peer-review under responsibility of the University of Oviedo

Keywords: Laser sintering metal, Fatigue, Block loadings, Functional materials;

1. Introduction

Selective laser melting (SLM) is a laser based rapid manufacturing technology that builds metal parts layer by-layer using metal powders and a computer controlled laser. According, Abe et al. [1] and Santos et al. [2] a high power laser

* Corresponding author. Tel.: 351 244 820 300.
E-mail address: ccapela@ipleiria.pt

Peer-review under responsibility of the University of Oviedo
doi:10.1016/j.proeng.2016.08.874

is used to fuse metallic powder particles, doing a scan of the transversal cross sections of the final component generated from a CAD model. Laser energy and scan speed must be adequately combine in order to continuous melting. The delivered energy produced continuous molten tracks by means of the complete melting of the powder, leading to coherent sintered tracks after solidification. This technique is increasingly used in automotive, aerospace, medical and of injection molds industries, to obtain components with complex shapes. Abundant literature has been previous reported on the scope of SLM using different metal powders, for instance, Simchi et al. [3] and, Kruth et al. [4] use iron-base alloys, Mumtaz et al. [5] nickel-base alloys, Gu et al. [6] copper-base alloys, Osakada et al. [7] titanium-base alloys.

SML products could show characteristic cast structure, with high superficial roughness, presence of porosity, heterogeneous microstructure and thermal residual stresses, resulting in mechanical properties which can be improved by additional post-processing treatments. Since SML can be used to manufacture functional components, it is essential a good characterization of the sintered parts to control final integrity of the parts, and to warranty that the components fulfill final functional requirements. As indicated by Simchi et al. [8] both powder characteristics (e.g., particle shape, size and its distribution, and component ratio) and processing parameters (e.g., laser power, scan speed, scan line spacing, and powder layer thickness) influence the densification level and the attendant microstructures of SLM-processed materials. Mechanical properties of sintered components are mainly affected by parameters, such as: porosity, surface roughness, scan speed, layer thickness, and residual stresses. A major drawback was obtained by Shiomi et al. [9], Murr et al. [10], Gorny et al. [11] and Vilaro et al. [12], consequence of the occurrence of pores originating from initial powder contaminations, evaporation or local voids after powder-layer deposition, which act as stress concentrators leading to failure. Especially effect was found by Brandl et al. [13] under fatigue loading.

The focus of this work is to produce and investigate the fatigue performance of hybrid specimens obtained by sintering laser of maraging steel implants into hot working tools and stainless steels substrates. The fatigue tests under constant amplitude and block loadings were carried out. Failure mechanisms and interfaces microstructures were detailed analysed.

2. Materials and testing

Experimental tests were performed in round specimens with the geometry and dimensions shown in Fig. 1. A high power laser was used to fuse steel powder particles layer by-layer in axial direction Fig. 1a). Two types of samples were prepared: single sintered specimens (all specimen is done by laser sintering technique) and two materials hybrid samples, in which one half part is an implant made laser sintered steel powder deposed on other half part machined substrate in other steel (as shown in Fig.1b). Powder particles to produce sintering laser parts was the maraging steel AISI 18Ni300, while the substrates of hybrid specimens were machined alternatively in two materials: the steel for hot work tools AISI H13 and the stainless steel AISI 420. Geometry and dimensions of the specimens are indicated in Fig. 1c). Table 1 show the chemical composition of the three materials, according with the manufacturers. Table 2 show the material design composition of the three materials compositions used in present study.

Table 1. Chemical composition of the materials.

Steel	C	Ni	Co	V	Mo	Ti	Al	Cr	P	Si	Mn	Fe
18Ni300	0.01	18.2	9.0	-	5.0	0.6	0.05	0.3	0.01	0.1	0.04	Balance
1.2344	0.40	-	-	0.94	1.30	-	-	5.29	0.017	1.05	0.36	Balance
1.2083	0.37	-	-	0.17	-	-	-	14.22	0.021	0.64	0.37	Balance

The samples were synthesized by Lasercusing®, with layers growing towards the application of load on the mechanical tests. The equipment for sintering is of the mark "Concept Laser" and model "M3 Linear". This apparatus comprises a laser type Nd: YAG with a maximum power of 100 W in continuous wave mode and a wavelength of 1064 nm. The samples were manufactured using the sintering scan speed of 200 mm/s. The test series are identified by the sample code followed by the scan speed.

The fatigue tests were carried out in tension at room temperature using a 10 kN capacity Instron EletroPuls E10000 machine, at constant amplitude and block sinusoidal load wave was applied with a frequency within the range 15–20

Hz and stress ratios of R = 0. All tests were performed under load control. The machine was equipped with grips specially prepared for the tests, as is shown in Fig. 2. Tensile tests were performed with the same machine at room temperature using a testing speed of 2 mm/min.

Variable amplitude tests were carried out using a reference block loading, composed by three blocks with stress ratio of R = 0, applied during 1000 of cycles for each one. Fig.3 shows schematically the sequence of the stress range applied during each block, which was repeated until final failure.

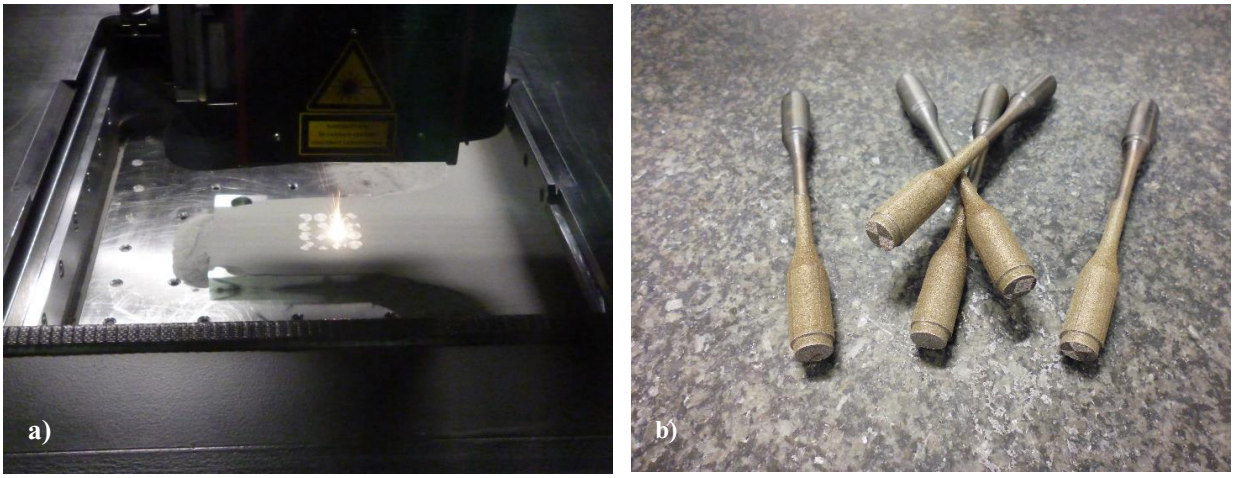

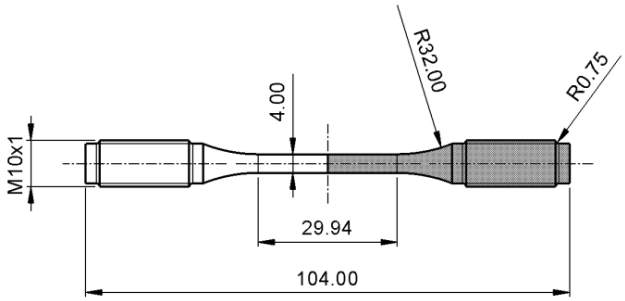

c)

Fig. 1. (a) Laser processing; (b) Hybrid specimens;(c) Geometry and dimensions of the specimens.

Table 2. Samples materials design.

Sample design	Sample code	Material A	Material B
Sintered	ST	18Ni300 Sintered power	18Ni300 Sintered power
Hybrid	ST/HS	18Ni300 Sintered power	1.2344 Hot working steel
Hybrid	ST/SS	18Ni300 Sintered power	1.2083 Stainless steel

3. Results and discussion

3.1. Metallography and porosity

Cross and long sectioning of the samples were prepared for metallographic analysis in order to identify the microstructure of the different zones, as well as the presence of porosity. The samples were prepared according to

standard metallographic practice ASTM E407-99. To observe the microstructure of the entirely sintered steel samples it was performed a chemical attack Picral (picric acid solution 4% in ethyl alcohol) for two minutes. For the observation of all the other material formulations it was added 1% hydrochloric acid into the Picral mixture and then it was carried out a second attack immersing the samples for 20 seconds. After prepared, the samples were observed using the microscope Leica DM4000 M LED.

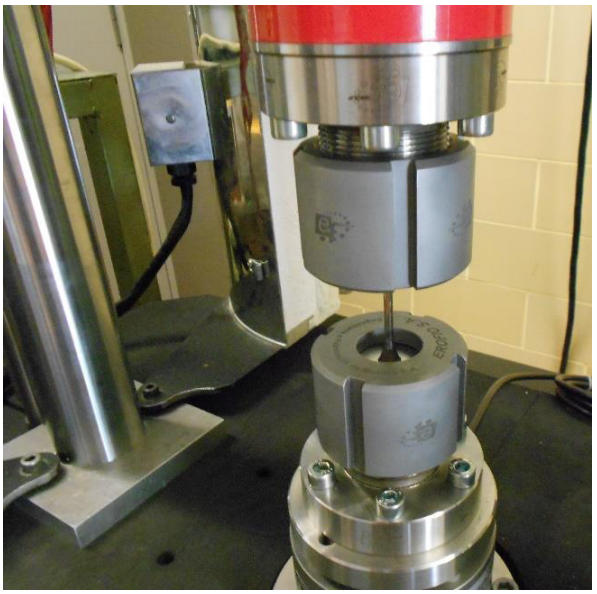

Fig. 2. Electropulse machine and grips.

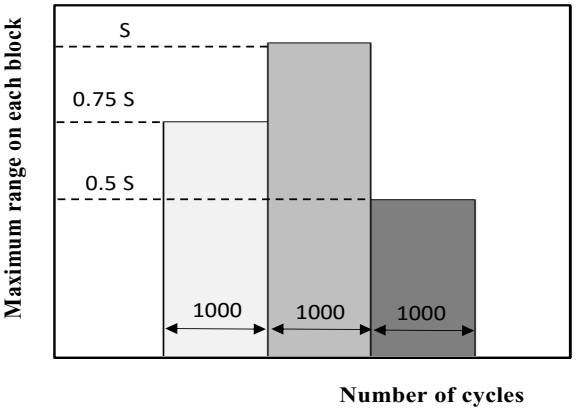

Fig. 3. Schematic presentation of the block loadings.

The images of microstructures were obtained in the sintered material and in interface region of hybrid biomaterial parts. Figs. 4 a) and b) show exemplary metallography in longitudinal sections of the single sintered material and of the interface region on hybrid samples, respectively. Fig.4a) shows elongated grains are observed with about 150 μm long and the abundant presence of small porosities with average diameter about 20 μm. Figs. 4b) shows a metallography in longitudinal section for a ST/SS hybrid specimen in interface region. The substrate material has a corrugated region caused by melting in the first laser pass. In 2083 steel it is observed a black zone which seems to

indicate a higher concentration of carbon and the zone near the interface is white indicating that have been a decarburization.

The quantification of the level of porosity was done by analysing the images contrast between the pores and the base material in the photographs by optical microscopy using image processing software Image J. From photographs obtained by optical microscopy (Fig. 5a)) the program creates a border with a blank line (Fig. 5b)) and afterwards calculates the area of each of these zones. The sum of all these areas gives the total porosity of the image. The values of porosity in percentage obtained was 0.74±0.09.

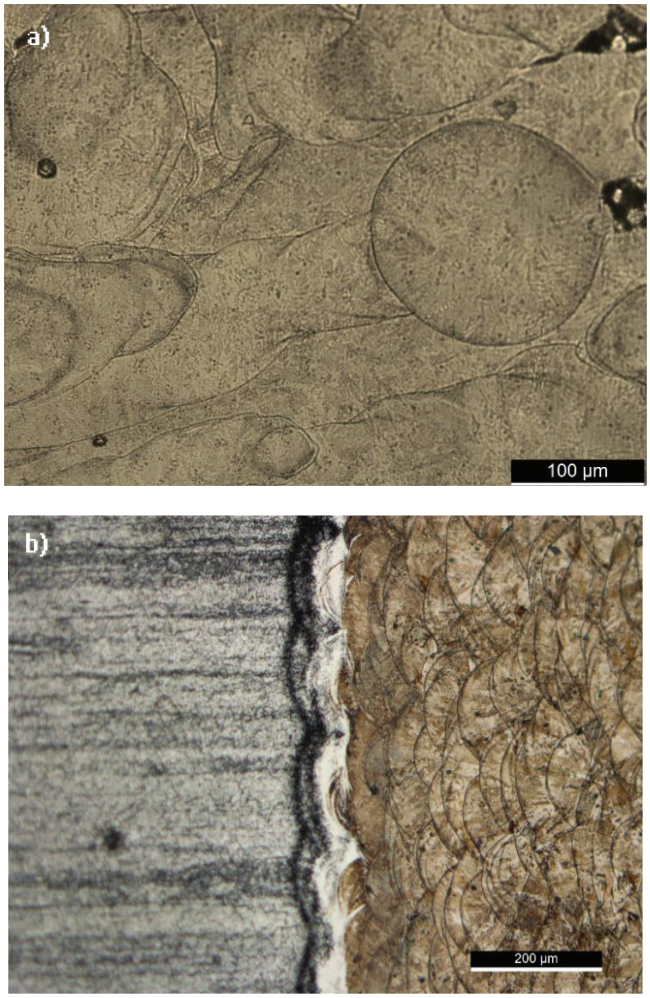

Fig. 4. Metallography's in longitudinal sections: (a) Sintered region; (b) Hybrid specimen interface.

3.2. Fatigue results

Tensile tests were performed in order to obtain basic mechanical properties. Ultimate strength was calculated using peak load. The stiffness modulus was obtained by linear regression of the stress-strain curves considering the larger range corresponding to a correlation coefficient higher than 0.995%. Table 3 summarizes the mechanical properties obtained for single sintered specimens and for hybrid parts.

The fatigue tests were carried out in tension at constant amplitude and block sinusoidal load. The fatigue results obtained under constant amplitude sinusoidal pulsating tensile loading, analyzed in terms of the stress range against

the number of cycles to failure, are presented in Fig. 6 for single sintered material (ST samples) and the ST/HS hybrid biomaterial parts. The analysis of the figure indicates that for short lives fatigue strength of the two series is similar. However, for longer life, the fatigue strength of hybrid specimens is progressively less than that of the fully sintered samples achieving a reduction in the order of 30% for $N = 5x10^5$ cycles.

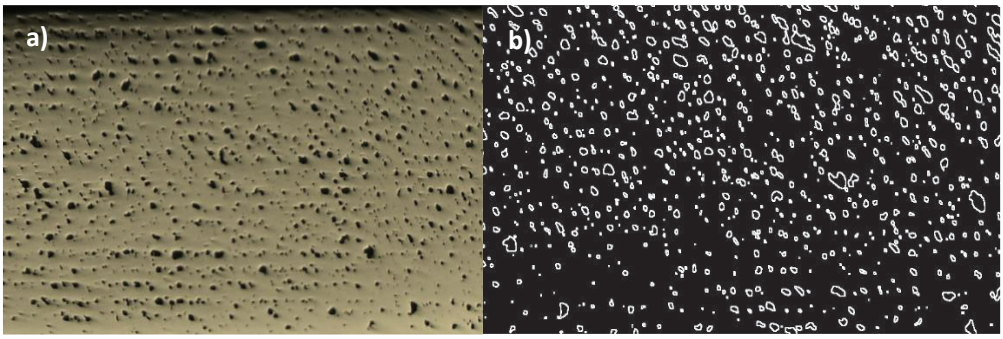

Fig. 5. Porosity images: (a) optical microscopy (b) Image J analysis.

Table 3. Mechanical properties.

Sample code	Young`s Modulus, GPa	Tensile Strength, MPa	Strain at failure, %
ST	168±29	1147±13	5.12±0.001
ST/HS	181±6	1139±12	4.6±0.03
ST/SS	163±7	1144±10	4.9±0.08

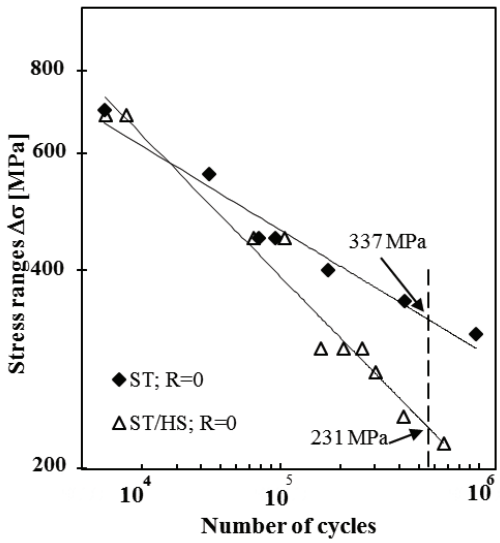

Fig. 6. S-N curves for constant amplitude tests for ST and ST/HS samples.

Variable amplitude loading fatigue results were analyzed using the known Miner`s law. Figs. 7 compare the equivalent stress range obtained from the Miner`s law and the experimental results obtained from constant amplitude tests for hybrid ST/SS specimens. From the analysis of this figure is can be concluded that Miner`s law is adequate to

predate fatigue life in hybrid components with sintered implants, despite having been observed a tendency to be conservative for long life.

Finally, a fracture surface analysis was performed with a scanning electron microscope (Philips XL30). Fig. 8 shows two SEM images. The fracture surface analysis showed that the crack initiated on the specimen's surface, and propagated through the cross section. In many cases it was observed a multi-nucleation as shown in Fig. 8a). Brittle crack propagation was the main mechanism observed in all cases. Fig. 8b) is a representative image, showing the initiation at the surface and the brittle crack propagation.

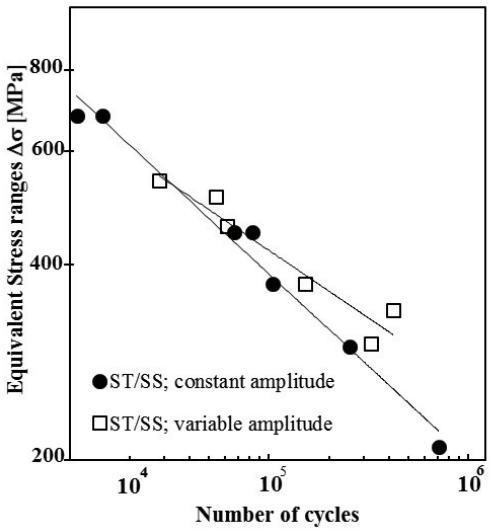

Fig. 7. Comparison of fatigue lives for constant and variable amplitude tests, based on the Miner`s law. ST/SS specimens.

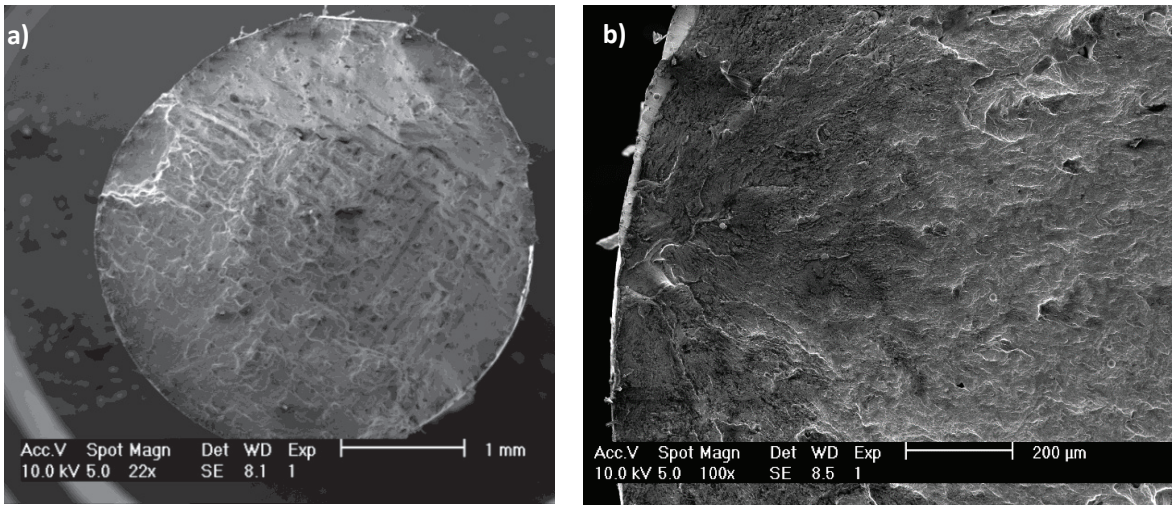

Fig. 8. SEM observations. a) Multi-nucleation; b) Initiation at the surface and propagation.

4. Conclusions

Present work studied the fatigue response of single laser sintered specimens and two materials hybrid formulations. The main conclusions are:

- Tensile properties of single laser sintered parts and two materials hybrid parts were quite similar;
- Fatigue strength of hybrid parts is quite similar to that of single sintered specimens for short lives, but tends to became significant lower for long lives.
- The fatigue tests under block loadings indicate that the application of Miner's law is adequate for engineering predictions of fatigue life in hybrid components with sintered implants.

Acknowledgements

The authors would like to acknowledge the sponsored by FEDER funds through the program COMPETE and national funds through FCT–Fundação para a Ciência e a Tecnologia, under the project number 016713 (PTDC/EMS-PRO/1356/2014) and also EROFIO S.A., Batalha, Portugal, by the supply of the materials and samples used this project.

References

[1] - F. Abe, K. Osakada, M. Shiomi, K. Uematsu, and M. Matsumoto, The Manufacturing of Hard Tools from Metallic Powders by Selective Laser Melting, J. Mater. Process. Technol. 111(1–3) (2001) 210–213.
[2] - E.C. Santos, M. Shiomi, K. Osakada, and T. Laoui, Rapid Manufacturing of Metal Components by Laser Forming, Int. J. Mach. Tools Manuf. 46(12–13) (2006) 1459–1468.
[3] - A. Simchi and H. Pohl, Direct Laser Sintering of Iron-Graphite Powder Mixture, Mater. Sci. Eng. A Struct. Mater. Prop. Microstruct. Process.383(2) (2004) 191–200.
[4] - J.P. Kruth, L. Froyen, J. Van Vaerenbergh, P. Mercelis, M. Rombouts, and B. Lauwers, Selective Laser Melting of Iron-Based Powder, J. Mater. Process. Technol. 149(1–3) (2004) 616–622.
[5] - K.A. Mumtaz, P. Erasenthiran, and N. Hopkinson, High Density Selective Laser Melting of Waspaloy (R), J. Mater. Process. Technol. 195(1–3) (2008) 77–87.
[6] - D.D. Gu and Y.F. Shen, Development and Characterisation of Direct Laser Sintering Multicomponent Cu Based Metal Powder, Powder Metall. 49(3), (2006) 258–264.
[7] - K. Osakada and M. Shiomi, Flexible Manufacturing of Metallic Products by Selective Laser Melting of Powder, Int. J. Mach. Tools Manuf. 46(11) (2006) 1188–1193.
[8] A. Simchi, F. Petzoldt, H. Pohl, Direct metal laser sintering : Material considerations and mechanisms of particle : Rand tooling of powdered metal parts, Int. J. Powder Metall. 37 (2001) 49–61.
[9] Shiomi, M., Osakada, K., Nakamura, K., Yamashita, T., Abe, F., Residual stress within metallic model made by selective laser melting process, CIRP Ann – Manuf Tech, 53(1) (2004) 195–198.
[10] Murr, L.E., Gaytan, S.M., Ceylan, A., Martinez, E., Martinez, J.L., Hernandez, D.H., et al., Characterization of titanium aluminide alloy components fabricated by additive manufacturing using electron beam melting, Acta Mater. 58(5) (2010) 1887–1894.
[11] Gorny, B., Niendorf, T., Lackmann, J., Thöne, M., Tröster, T., Maier, H.J., In situ characterization of the deformation and failure behaviour of non-stochastic porous structures processed by selective laser melting, Mater Sci Eng. A528 (27) (2011) 962–967.
[12] Vilaro, T., Colin, C., Bartout, J.D., As-fabricated and heat-treated microstructures of the Ti–6Al–4V alloy processed by selective laser melting, Metall Mater Trans A. 42A(10) (2011) 3190–3199.
[13] Brandl, E., Heckenberger, U., Holzinger, V., Buchbinder, D., Additive manufactured AlSi10Mg samples using selective laser melting (SLM): microstructure, high cycle fatigue, and fracture behaviour, Mater Design, 34 (2012) 159–169.